

## Facile Synthesis of Z-Scheme Fe-nPPy/BiOI Nanocomposite for Enhanced Visible Light Driven Photocatalytic Activity

Rajesh Kumar<sup>a,b</sup>, Rituporn Gogoi<sup>a</sup>, Kajal Sharma<sup>a</sup>, Astha Singh<sup>a</sup>, Prem Felix Siril<sup>a\*</sup>

<sup>a</sup> School of Chemical Sciences, Indian Institute of Technology Mandi, Mandi, Himachal Pradesh-175005, India

<sup>b</sup> Govt. College Kullu, Himachal Pradesh- 175101, India

\*Corresponding author: [prem@iitmandi.ac.in](mailto:prem@iitmandi.ac.in)

### Table of Content:

Sr. No.	Contents	Page
1	<b>Fig. S1:</b> XRD patterns (a) and FTIR spectra (b) of the synthesized nanocomposites	S-2
2	<b>Fig. S2:</b> XPS survey spectra of synthesized nanocomposites.	S-2
3	<b>Fig. S3:</b> Deconvoluted Fe2p XPS spectra of (a) Fe-nPPy and (b) Fe-nPPy/BiOI-3	S-3
4	<b>Table S1:</b> Surface elemental composition of Fe-nPPy/BiOI-3 as per XPS survey spectra.	S-3
5	<b>Fig. S4:</b> SEM images (a & b) of BiOI and Fe-nPPy (c & d).	S-4
6	<b>Fig. S5:</b> (a) Adsorption profiles of CV dye over Fe-nPPy/BiOI catalysts.	S-5
7	<b>Fig. S6:</b> Variation in the UV-Vis absorbance spectra with time of: (a) CV dye and (b) Tetracycline (TC) using Fe-nPPy/BiOI-3 photocatalyst under visible light irradiation.	S-5
8	<b>Table S2:</b> Comparison of the photocatalytic activity of the Fe-nPPy/BiOI-3 with some other hybrid composites for the degradation of Crystal violet (CV) dye and Tetracycline (TC) under visible light irradiation.	S-6
9	<b>Fig. S7:</b> XRD patterns of fresh and recovered Fe-nPPy/BiOI-3 photocatalyst after three cycles	S-7
10	<b>Fig. S8:</b> (a) Time-dependent variation of the UV-visible absorbance spectra of NBT during visible light irradiation in presence of Fe-nPPy/BiOI-3 photocatalyst and (b) the respective kinetic curve.	S-8
11	<b>Fig. S9:</b> (a) Mott-Schottky plots of (a) BiOI and (b) Fe-nPPy.	S-9
12	<b>Fig. S10:</b> XPS spectra of Fe-nPPy/BiOI-3 before and after photocatalysis for Bi-4f and N-1s respectively.	S-10
13	<b>References</b>	S-11

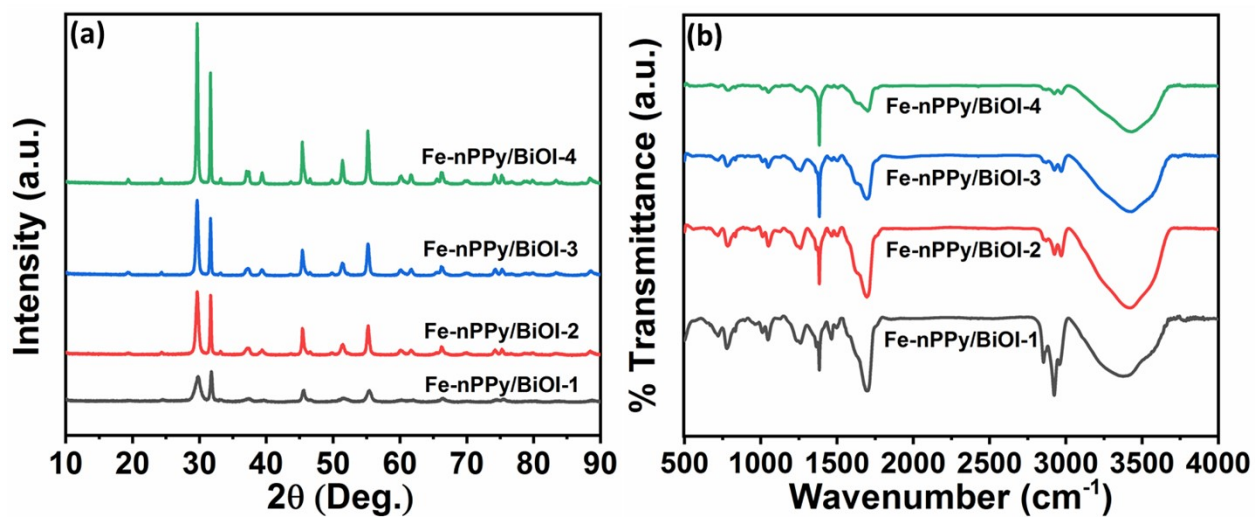


Fig. S1: (a) XRD patterns and (b) FTIR spectra of the synthesized nanocomposites.

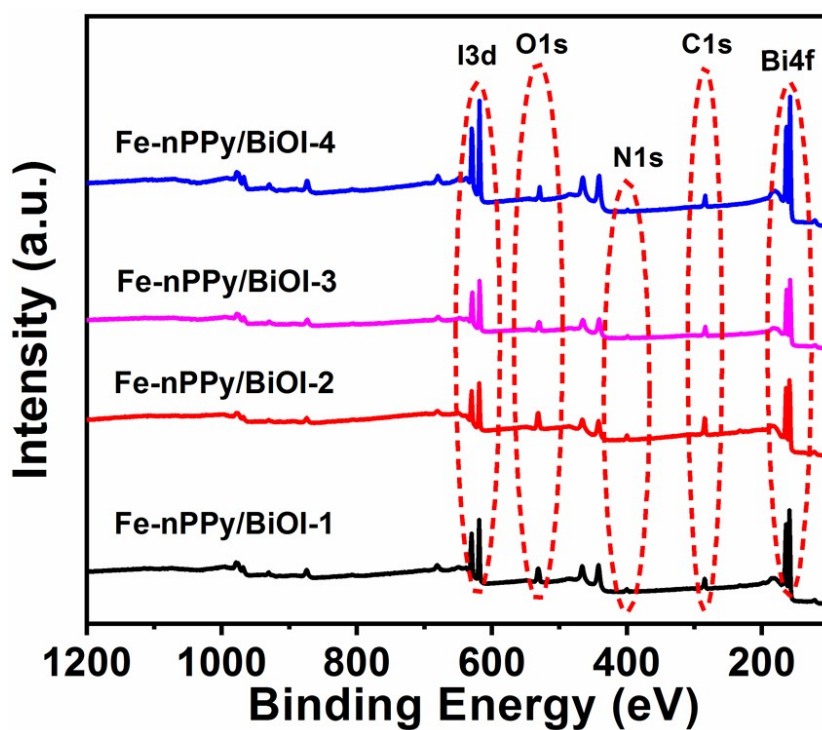


Fig. S2: XPS survey spectra of as synthesized nanocomposites.

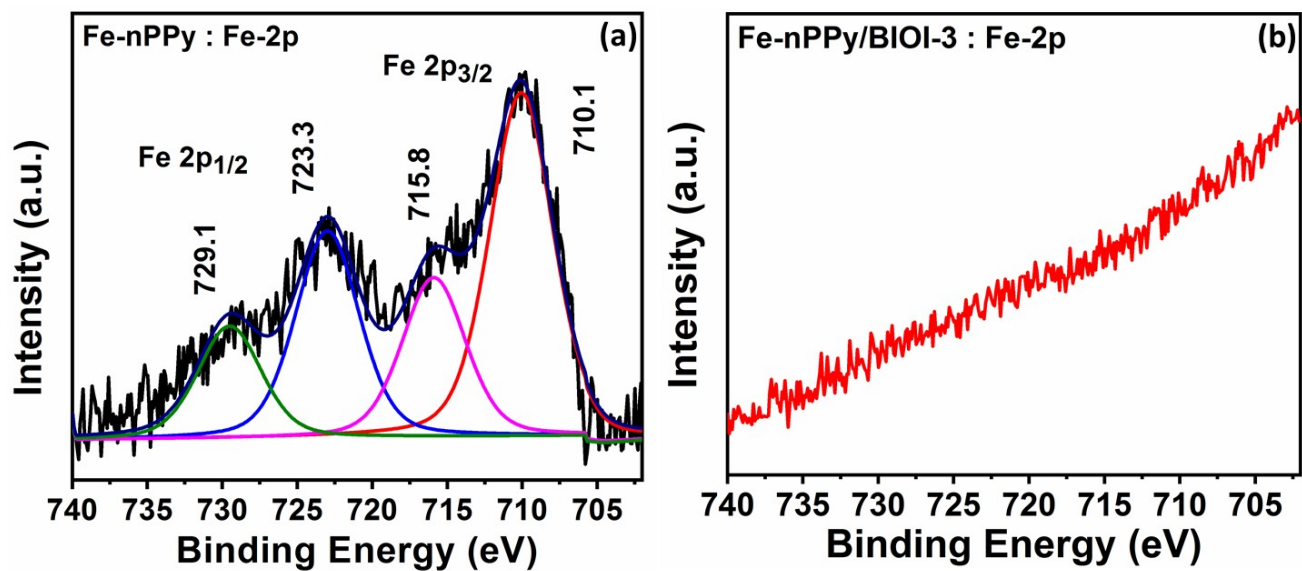
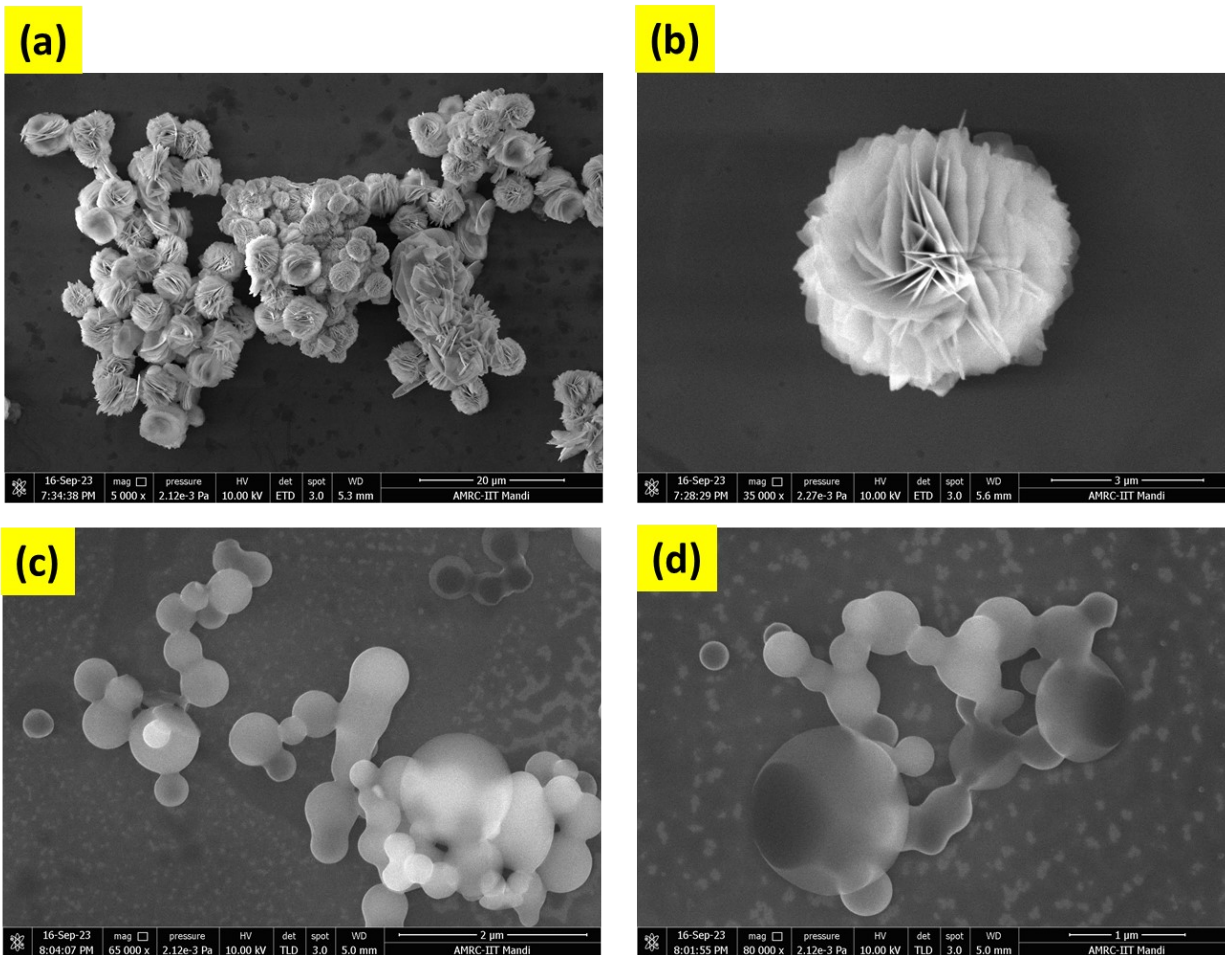


Fig. S3: Deconvoluted Fe2p XPS spectra of (a) Fe-nPPy and (b) Fe-nPPy/BiOI-3.

Table S1: Surface elemental composition of Fe-nPPy/BiOI-3 as per XPS survey spectra.

Name	Peak BE	FWHM eV	Area (P) CPS.eV	Atomic %	Q	SF
I3d	619.75	1.58	2755213.41	7.27	1	42.416
Bi4f	159.88	2.52	5469514.21	11.55	1	38.304
C1s	285.87	3.08	608732.95	53.19	1	1
O1s	531.23	4.23	596396.4	21.53	1	2.881
N1s	400.79	3.3	110187.25	6.2	1	1.676
Fe2p	720.08	0.56	29798.18	0.25	1	14.353



**Fig. S4:** FESEM images of: (a & b) BiOI and (c & d) Fe-nPPy.

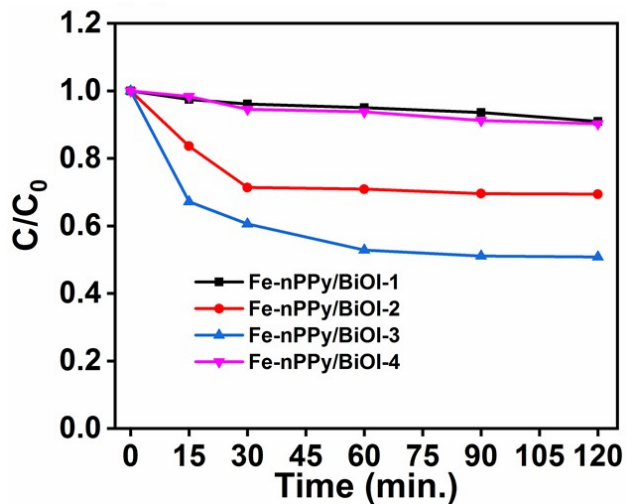


Fig. S5: (a) Adsorption profiles of CV dye over Fe-nPPy/BiOI catalysts.

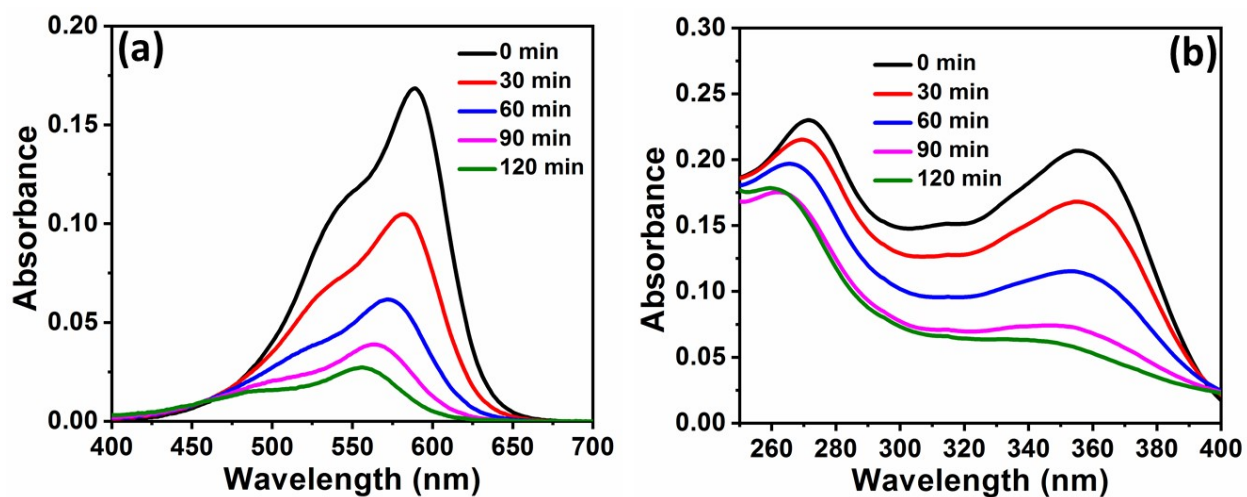


Fig. S6: Variation in the UV-Vis absorbance spectra with time of: (a) CV dye and (b) Tetracycline (TC) using Fe-nPPy/BiOI-3 photocatalyst under visible light irradiation.

**Table S2:** Comparison of the photocatalytic activity of the Fe-nPPy/BiOI-3 with some other hybrid composites for the degradation of Crystal violet (CV) dye and Tetracycline (TC) under visible light irradiation.

Photocatalyst	Pollutant, concentration (ppm)	Catalyst amount (mg/mL)	Visible light source	Synthesis method	Removal (%)	Time (min.)	References
g-C <sub>3</sub> N <sub>4</sub> /Ag <sub>3</sub> VO <sub>4</sub>	CV, 20	1	500 W Xe arc lamp	ultrasound-assisted	85	150	[1]
F-TiO <sub>2</sub> (B)/fullerene	CV, 30	0.1	500 W halogen lamp	Ballmill + hydrothermal	77.2	120	[2]
SrFeO <sub>3-x</sub> /g-C <sub>3</sub> N <sub>4</sub>	CV, 10	0.1	150 W Xe arc lamp	sintering method	99.9	720	[3]
Gd doped BiFeO <sub>3</sub>	CV, 20	0.2	250 W mercury lamp	auto-combustion method	84.5	150	[4]
Fe-nPPy/BiOI-3	CV, 10	0.5	192 W white LEDs	RT co-precipitation	84.0	120	Current work
Fe <sub>3</sub> O <sub>4</sub> @TiO <sub>2</sub> -Co	TC, 50	0.2	300 W Xe arc lamp	Facile reduction method	92.4	120	[5]
Ag/AgBr/AgI@SiO <sub>2</sub> aerogel	TC, Not known	0.3	300 W Xe arc lamp	Supercritical drying process	79.5	50	[6]
PPy-BiOI	TC, 30	1	Not known	Co-precipitation	61	300	[7]
Fe-nPPy/BiOI-3	TC, 20	1	192 W white LEDs	RT co-precipitation	74	120	Current work

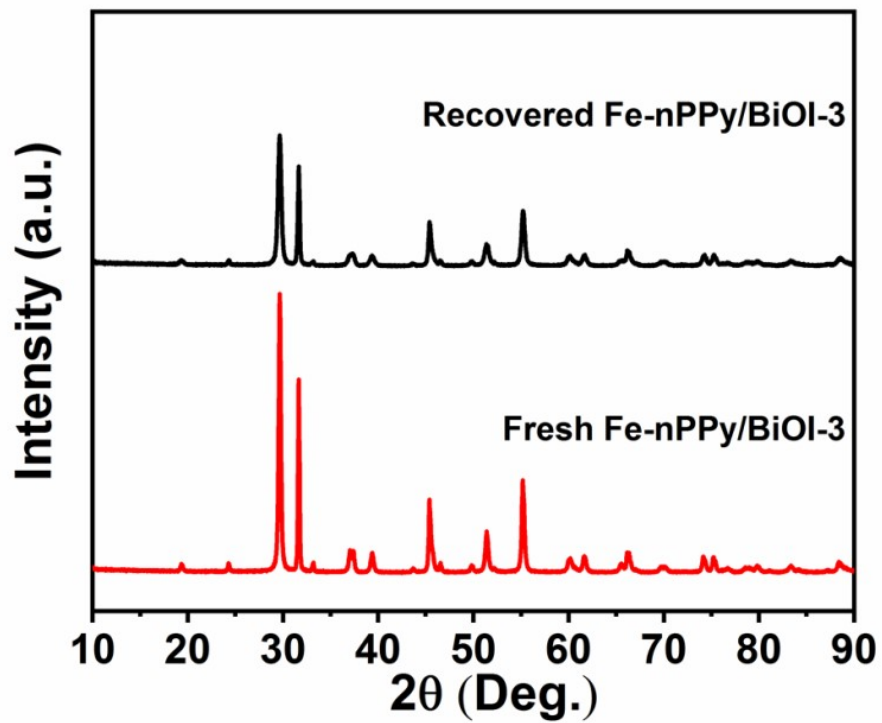
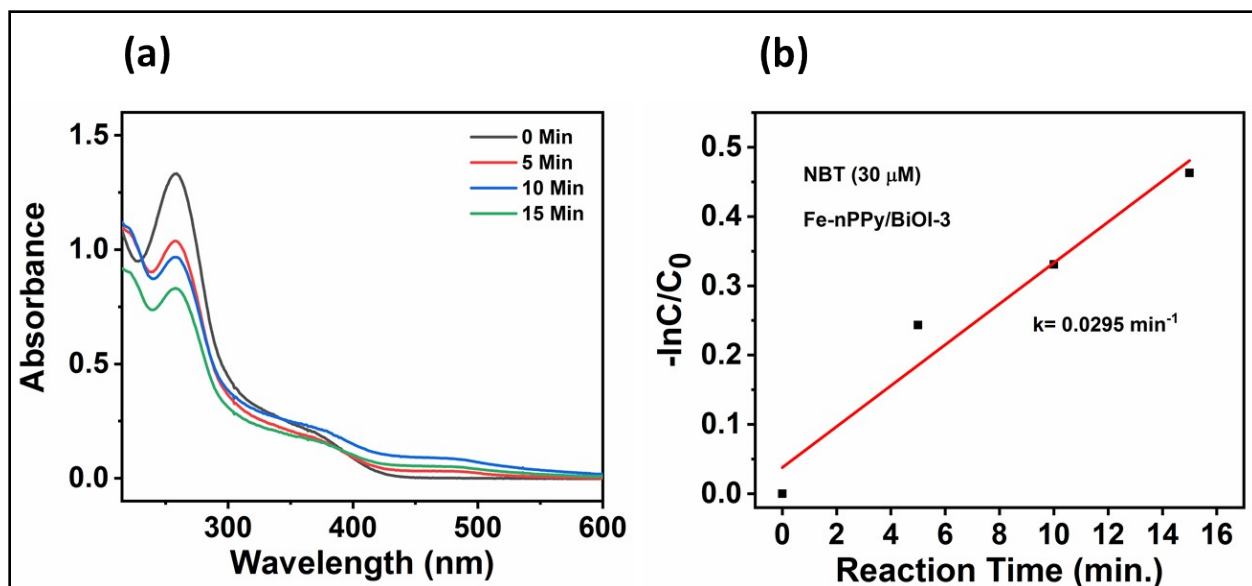


Fig. S7: XRD patterns of fresh and recovered Fe-nPPy/BiOI-3 photocatalyst after three cycles



**Fig. S8:** (a) Time-dependent variation of the UV-visible absorbance spectra of NBT during visible light irradiation in presence of Fe-nPPy/BiOI-3 photocatalyst and (b) the respective kinetic curve.

$$\text{Concentration of } \bullet\text{O}_2^- \text{ radical} = k_{\text{NBT}} \times t \times C_{\text{initial}} \times 4$$

$$k_{\text{NBT}} = 0.0295 \text{ min}^{-1} \text{ (loss kinetic constant of NBT)}$$

$$t = 15 \text{ min (the light exposure time)}$$

$$C_{\text{initial}} = 30 \text{ } \mu\text{M (NBT initial concentration)}$$

4 is the constant coefficient between the reaction of NBT and  $\bullet\text{O}_2^-$



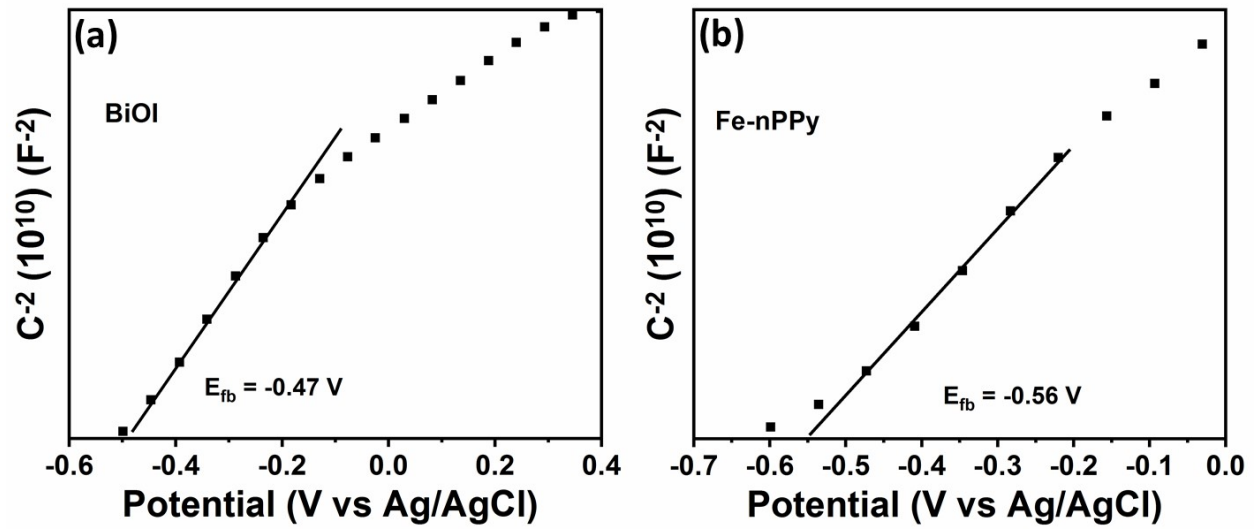


Fig. S9: (a) Mott-Schottky plots of (a) BiOI and (b) Fe-nPPy.

We have used the following relation for conduction band calculation;

$$E \text{ (RHE)} = E \text{ (Ag/AgCl)} + 0.197 \text{ (at pH = 7)}$$

Further, valence band edge is calculated by applying the relation;

$$E_{CB} = E_{VB} - E_g \text{ (} E_g \text{ is calculated from DRS studies for BiOI and Fe-nPPy)}$$

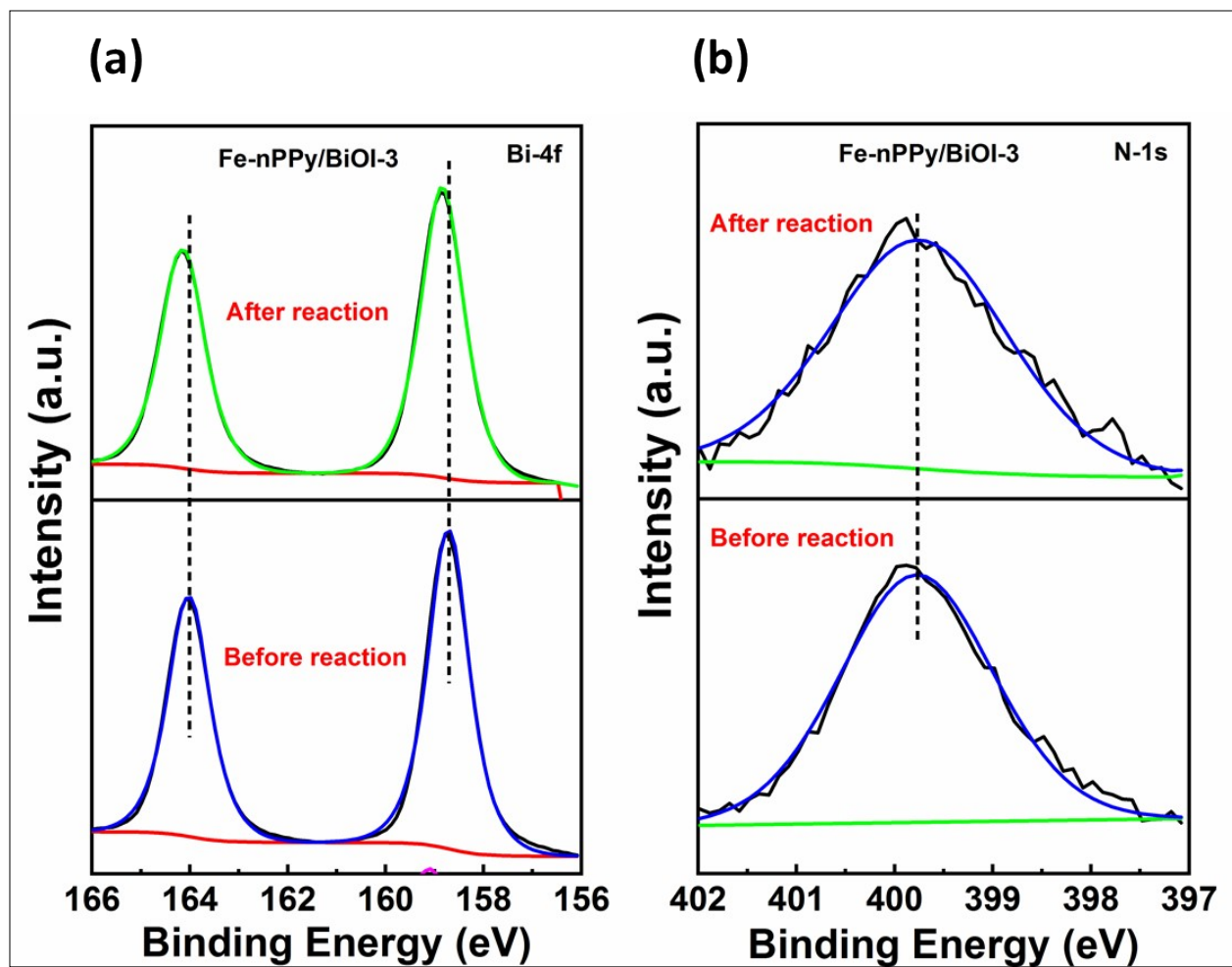


Fig. S10: XPS spectra of Fe-nPPy/BiOI-3 before and after photocatalysis for Bi-4f and N-1s respectively.

## References:

- S[1]:** S. Wang, D. Li, C. Sun, S. Yang, Y. Guan, H. He, Synthesis and characterization of g-C<sub>3</sub>N<sub>4</sub>/Ag<sub>3</sub>VO<sub>4</sub> composites with significantly enhanced visible-light photocatalytic activity for triphenylmethane dye degradation, *Appl. Catal. B Environ.* 144 (2014) 885–892. <https://doi.org/10.1016/j.apcatb.2013.08.008>
- S[2]:** Y. Panahian, N. Arsalani, R. Nasiri, Enhanced photo and sono-photo degradation of crystal violet dye in aqueous solution by 3D flower like F-TiO<sub>2</sub>(B)/fullerene under visible light, *J. Photochem. Photobiol. A Chem.* 365 (2018) 45–51. <https://doi.org/10.1016/J.JPHOTOCHEM.2018.07.035>
- S[3]:** H.P. Lin, C.C. Chen, W.W. Lee, Y.Y. Lai, J.Y. Chen, Y.Q. Chen, J.Y. Fu, Synthesis of a SrFeO<sub>3-x</sub>/g-C<sub>3</sub>N<sub>4</sub> heterojunction with improved visible-light photocatalytic activities in chloramphenicol and crystal violet degradation, *RSC Adv.* 6 (2016) 2323–2336. <https://doi.org/10.1039/c5ra21339h>
- S[4]:** S. Kossar, I.B.S. Banu, N. Aman, R. Amiruddin, Investigation on photocatalytic degradation of crystal violet dye using bismuth ferrite nanoparticles, *J. Dispers. Sci. Technol.* 42 (2021) 2053–2062. <https://doi.org/10.1080/01932691.2020.1806861>
- S[5]:** Tan, Q., Zhang, W., ... Niu, Li, 2023. Magnetically induced construction of core-shell architecture Fe<sub>3</sub>O<sub>4</sub>@TiO<sub>2</sub>-Co nanocomposites for effective photocatalytic degradation of tetracycline. *New Journal of Chemistry* 47, 15951–15962. doi:10.1039/d3nj02080k
- S[6]:** Ma, C., Shi, F., Liu, J., Li, T., Zhu, K., Liu, J., ... Xiao, J. (2023, June 1). Construction of a novel Ag/AgBr/AgI@SiO<sub>2</sub> composite aerogel with controlled pore structure: Efficient removal of tetracycline by adsorption/photocatalysis synergism under visible light irradiation. *Journal of Environmental Chemical Engineering*. Elsevier Ltd. <https://doi.org/10.1016/j.jece.2023.110157>
- S[7]:** Xu, J., Hu, Y., Zeng, C., Zhang, Y., & Huang, H. (2017). Polypyrrole decorated BiOI nanosheets: Efficient photocatalytic activity for treating diverse contaminants and the critical role of bifunctional polypyrrole. *Journal of Colloid and Interface Science*, 505, 719–727. <https://doi.org/10.1016/j.jcis.2017.06.054>